

# Regulation of Connexin43 Function and Expression by Tyrosine Kinase 2\*

Received for publication, March 11, 2016, and in revised form, May 16, 2016. Published, JBC Papers in Press, May 27, 2016, DOI 10.1074/jbc.M116.727008

Hanjun Li, Gaelle Spagnol, Li Zheng, Kelly L. Stauch, and Paul L. Sorgen<sup>1</sup>

From the University of Nebraska Medical Center, Omaha, Nebraska 68105

Connexin43 (Cx43) assembly and degradation, the regulation of electrical and metabolic coupling, as well as modulating the interaction with other proteins, involve phosphorylation. Here, we identified and characterized the biological significance of a novel tyrosine kinase that phosphorylates Cx43, tyrosine kinase 2 (Tyk2). Activation of Tyk2 led to a decrease in Cx43 gap junction communication by increasing the turnover rate of Cx43 from the plasma membrane. Tyk2 directly phosphorylated Cx43 residues Tyr-247 and Tyr-265, leading to indirect phosphorylation on residues Ser-279/Ser-282 (MAPK) and Ser-368 (PKC). Although this phosphorylation pattern is similar to what has been observed following Src activation, the response caused by Tyk2 occurred when Src was inactive in NRK cells. Knockdown of Tyk2 at the permissive temperature (active v-Src) in LA-25 cells decreased Cx43 phosphorylation, indicating that although activation of Tyk2 and v-Src leads to phosphorylation of the same Cx43CT residues, they are not identical in level at each site. Additionally, angiotensin II activation of Tyk2 increased the intracellular protein level of Cx43 via STAT3. These findings indicate that, like Src, Tyk2 can also inhibit gap junction communication by phosphorylating Cx43.

Gap junctions are integral membrane proteins that enable the direct cytoplasmic exchange of ions and low molecular weight metabolites (<1 kDa) between adjacent cells. They provide an intercellular pathway for the propagation and/or amplification of signal transduction cascades triggered by cytokines, growth factors, and other cell-signaling molecules involved in growth regulation and development. Gap junctions are formed by the apposition of connexons from adjacent cells, where each connexon is formed by six connexin proteins. Connexins are tetraspanning transmembrane proteins with intracellular N and C termini (CT).<sup>2</sup> There are 21 human isoforms, and although there is significant sequence homology among connexins, their major divergence occurs in the cytoplasmic domains. Connexin43 (Cx43), the most ubiquitously expressed

connexin isoform, has been well studied in terms of structure, function, and regulation (1).

Cx43 channels can be regulated by a variety of molecules and physiological conditions (e.g. Ca<sup>2+</sup>, pH, and intercellular voltage), including through phosphorylation (2, 3). All stages of the Cx43 life cycle (i.e. trafficking, assembly/disassembly, degradation, and channel gating (3)), as well as the regulation of electrical and metabolic coupling and of interactions with other proteins, involve phosphorylation. The Cx43CT is differentially phosphorylated on at least 20 residues, and significant progress has been achieved in characterizing the kinases involved (2, 4–6). Unfortunately, an understanding of the mechanism(s) by which Cx43 phosphorylation alters channel function is lacking. Several problems contributing to this difficulty include the transient nature of a particular CT phosphorylation state, the ability of many kinases to phosphorylate more than one CT residue, the ability of various kinases to phosphorylate the CT at the same time, and the inability to precisely control which residues are phosphorylated. Strategies employed to overcome these difficulties include the use of phospho-specific CT antibodies (7) and short CT phosphopeptides (8, 9). Also well appreciated is the use of Asp (or Glu) substitutions as a mimetic for phosphorylation (10, 11).

The negative charge of the phosphate could affect the permeability of ions through the pore, alter the structure of the transmembrane  $\alpha$ -helices to influence pore size, or modify the binding affinities of molecular partners involved in Cx43 regulation. Notably, if phosphorylation modifies protein interactions to affect the kinetics of channel assembly/disassembly or degradation, cell-to-cell communication will also be altered. Evidence has emerged that a phosphate can directly block the Cx43CT interaction with ZO-1 (9) and tubulin (8) or enhance the interaction with Nedd4 (12, 13). This information is critical because a particular cellular condition can be correlated with a specific Cx43 phosphorylation status to understand which proteins will and will not interact to affect regulation of Cx43. Numerous serine protein kinases have been identified as directly phosphorylating Cx43 (for review see Ref. 4); however, tyrosine-protein kinases have been limited to the well studied cases involving c- and v-Src-induced phosphorylation (14–18). In this study, we identified Cx43 as a novel substrate of tyrosine kinase 2 (Tyk2).

Tyk2, a JAK family member, is a ubiquitously expressed non-receptor tyrosine kinase. Tyk2 associates with the intracellular domains from a wide range of cytokine and growth factor receptors via its N-terminal FERM and SH2-like domains (19–21). This leads to recruitment and phosphorylation of STATs (22), which translocate to the nucleus where they induce transcription of genes involved in diverse biological processes (e.g.

\* This work was supported by National Institutes of Health Grants GM072631 and HL131712. The authors declare that they have no conflicts of interest with the contents of this article. The content is solely the responsibility of the authors and does not necessarily represent the official views of the National Institutes of Health.

<sup>1</sup> To whom correspondence should be addressed: Dept. of Biochemistry and Molecular Biology, University of Nebraska Medical Center, Omaha, NE 68198. Tel.: 402-559-7557; Fax: 402-559-6650; E-mail: psorgen@unmc.edu.

<sup>2</sup> The abbreviations used are: CT, C terminal; Cx43, connexin43; Tyk2, tyrosine kinase 2; RAS, renin-angiotensin system; Ang II, angiotensin II; ACE, angiotensin-converting enzyme; GJIC, gap junction intercellular communication; NRK, normal rat kidney.

## Tyk2 Phosphorylates Cx43

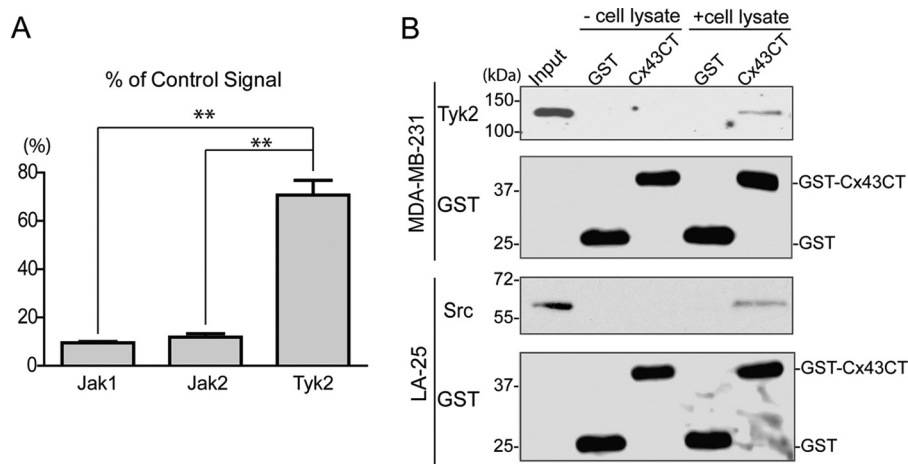


**FIGURE 1. Phosphorylation of the Cx43CT domain by JAK tyrosine kinases.** *A*, an *in vitro* kinase assay was performed using the catalytic domain of Jak1, Jak2, and Tyk2 to phosphorylate purified Cx43CT. The amount of Cx43CT phosphorylation was compared with a positive control peptide for each kinase (100% signal) (\*\*,  $p < 0.01$ ). *B*, purified GST (26 kDa) or GST-Cx43CT (42 kDa) bound on glutathione-agarose beads was incubated with or without MDA-MB-231 cell lysate (*top*), and the pulled down product was analyzed by Western blotting analysis using an anti-Tyk2 antibody. GST-Cx43CT pull-down of Src from LA-25 cell lysate was used as the positive control (*bottom*).

cellular proliferation and differentiation, inflammation, and defense against infection (23, 24)). Patients with nonfunctional Tyk2 display a number of immunodeficiency conditions and increased susceptibility to infections caused by defects in IFN $\alpha/\beta$ , IL-6, IL-10, IL-12, and IL-23 signaling (25). Tyk2-deficient mice display reduced responses to IFN $\alpha/\beta$  and IL-12 and a deficiency in STAT3 activation (26). The Tyk2/STAT3 axis has also been implicated in the induction of neuronal death in Alzheimer disease (27), as a biomarker for Crohn's disease (28), and in controlling allergic asthma (29). Marrero *et al.* (30) first showed that angiotensin II (Ang II) induces Tyk2 activation in rat aortic smooth muscle cells, a finding verified in other studies (31–34). The renin-angiotensin system (RAS) is a key signaling pathway associated with the pathogenesis of cardiovascular disease (35, 36). Increased Ang II levels are linked with an increased risk of ventricular arrhythmia, and treatment with angiotensin-converting enzyme (ACE) inhibitors has demonstrated survival benefits in congestive heart failure and myocardial infarction (37–39). A transgenic mouse model of RAS activation by overexpression of ACE restricted to the heart (ACE8/8) has normal ventricular structure; however, it exhibits cardiac oxidative stress, a high incidence of ventricular tachycardia, and subsequent sudden cardiac death. With no significant change in the Na<sup>+</sup> current, these observations were associated with down-regulation of Cx43 gap junction intercellular communication GJIC (40). Altered cardiac Cx43 protein level and change in cellular localization also have been observed in other models of RAS activation (hypertension, hypertrophy, and mechanical stress (41–44)). Here, we provide evidence of a relationship between Tyk2 activation by Ang II and Tyk2 phosphorylation of Cx43. Tyk2 decreased gap junction stability at the plasma membrane and, through STAT3 activation, increased the intracellular protein level of Cx43.

### Results

**Tyk2 Directly Interacts with and Phosphorylates the Cx43CT Domain**—Src is the only known tyrosine kinase to both directly phosphorylate the Cx43CT domain (pTyr-247 and pTyr-265)

and affect GJIC (45, 46). However, proteomic discovery mode mass spectrometry (MS) data identify other tyrosine residues (Tyr-267, Tyr-286, Tyr-301, and Tyr-313) as potential phosphorylation targets (see PhosphoSitePlus Website). Unfortunately, the kinases involved were not identified, and neither was the functional significance of phosphorylation at these sites. In this study, we focused on the JAK family of tyrosine kinases because of the potential direct link between Cx43 and RAS in the pathogenesis of cardiovascular disease (35, 36, 47, 48). An *in vitro* tyrosine phosphorylation screen performed by Eurofins Scientific (KinaseProfiler) found that Tyk2 phosphorylated purified Cx43CT<sup>236–382</sup> (Fig. 1A). JAK1 and JAK2, also JAK family members, had significantly less ability to phosphorylate the Cx43CT domain (JAK3 was not tested because it is not expressed in the heart). To confirm the interaction between Cx43 and Tyk2, purified GST-tagged Cx43CT<sup>236–382</sup> was immobilized on glutathione-Sepharose beads, and lysate from MDA-MB-231 cells that express Tyk2 (but not Cx43) was used in a pull-down assay (Fig. 1B). Tyk2 can be pulled down by GST-Cx43CT but not GST in MDA-MB-231 cells. Src was used as a positive control.

**Identifying the Cx43CT Tyrosine Residue(s) Phosphorylated by Tyk2**—Purified Cx43CT<sup>236–382</sup> was incubated *in vitro* with active Tyk2 (p-Tyk2, Life Technologies) as described previously (49, 50), and phosphorylation was confirmed using an anti-phosphotyrosine antibody (Fig. 2B). After trypsin digestion, Tandem MS/MS identified phosphorylation at Tyr-247, Tyr-265, Tyr-267, and Tyr-313 (Fig. 2A and Table 1). To confirm that tyrosine phosphorylation can occur at residues other than Tyr-247 and Tyr-265, the *in vitro* kinase assay was performed using the Cx43CT<sup>236–382</sup> (Y247,265F) (2YF) construct, and phosphorylation was detected with an anti-phosphotyrosine antibody (Fig. 2B). The data indicate that although a majority of Tyk2 phosphorylation occurs on Tyr-247 and Tyr-265 (of note, Tyr-247 and Tyr-265 phospho-specific antibodies will be used in the next sections to further characterize these sites), other tyrosine sites (*i.e.* Tyr-267 and Tyr-313) can be phosphorylated by Tyk2 *in vitro*.

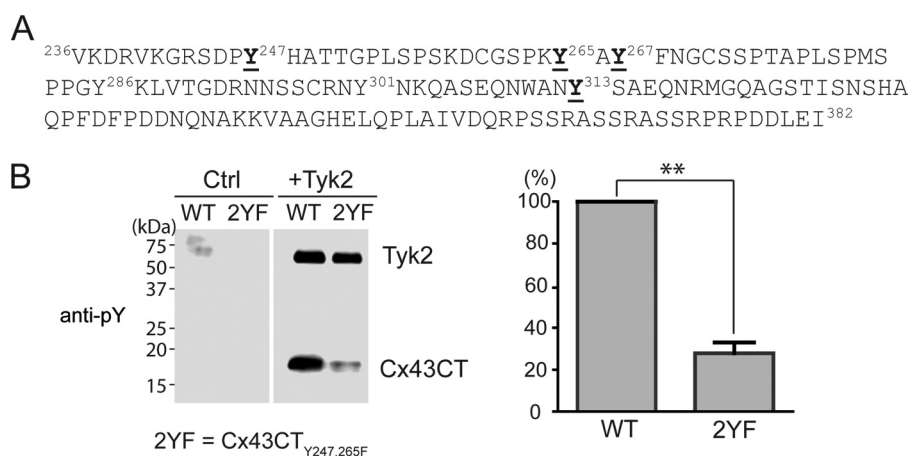


**FIGURE 2. Identification of the Cx43CT tyrosine residues phosphorylated by Tyk2.** *A*, sequence of the Cx43CT domain. The Cx43CT tyrosine residues identified from mass spectrometry to be phosphorylated by the Tyk2 catalytic domain *in vitro* are highlighted (*bold and underlined*). *B*, the same *in vitro* kinase assay as described in *A* was performed using wild-type Cx43CT<sup>236–382</sup> or a Y247,265F (2YF) mutant as substrate, and phosphorylation was detected by Western blotting using a general anti-phosphotyrosine antibody. The control (*Ctrl*) group did not contain Tyk2. The phosphotyrosine level was quantified using ImageJ software ( $n = 3$ , \*\*,  $p < 0.01$ ).

**TABLE 1**  
**Phosphotyrosine-containing peptides identified from mass spectrometry of the Cx43CT domain phosphorylated *in vitro* by Tyk2**

Peptide sequence	Start-end positions	Average Mascot Delta Ion Score	No. of phosphopeptides <sup>a</sup>	Actual peptide mass	Calculated +1H peptide mass	Phosphorylation site localization
GRSDP <sub>Y</sub> HATTGPLSPSK	242–258	15.35	4	1849.84	1850.84	Tyr-247
SDP <sub>Y</sub> HATTGPLSPSK	244–258	18.5	6	1636.72	1637.72	Tyr-247
GRSDP <sub>Y</sub> HATTGPLSPSKDc(carbamidomethyl)GSPK	242–264	9.37	2	2667.04	2668.05	Tyr-247
QASEQNWAN <sub>Y</sub> SAEQNR	304–319	13.7	2	1974.79	1975.79	Tyr-313
<sub>Y</sub> AYFNGc(carbamidomethyl)SSPTAPLSPm(oxidation)SPPGYK	265–287	7.14	1	2588.07	2588.07	Tyr-265
<sub>Y</sub> AYFNGc(carbamidomethyl)SSPTAPLSPm(oxidation)SPPGYK	265–287	13.8	1	2667.05	2668.05	Tyr-Y265, Tyr-267

<sup>a</sup> Peptides with a Mascot Delta Ion Score > 7 were used to obtain the average Mascot Delta Ion Score according to Savitski *et al.* (90).

*Tyk2 Phosphorylates Cx43 Residues Tyr-247 and Tyr-265 Leading to Decreased Stability of the Gap Junction Plaque in Normal Rat Kidney (NRK) Epithelial Cells*—To determine whether Tyk2 phosphorylation of Cx43 occurs in cells, we initially tested in NRK cells if Cx43 (endogenously expressed) and Tyk2 (not expressed; transiently transfected with a constitutively active construct, Tyk2<sub>V678F</sub>) colocalize (Fig. 3). The images suggest little to no colocalization in NRK cells that over-express active Tyk2. However, in those same NRK cells, Cx43 was significantly decreased at the plasma membrane. The data suggest that over-expressing active Tyk2 leads to the internalization of Cx43 from the plasma membrane.

Next, the tyrosine phosphorylation levels were evaluated in NRK cells using the only available Cx43 tyrosine phospho-specific antibodies, pTyr-247 and pTyr-265 (Fig. 4). Constitutively active Tyk2 increased both Tyr-247 and Tyr-265 phosphorylation levels as compared with controls (non-transfected cells). Importantly, the presence of active Tyk2 did not activate Src. Because MAPK and PKC have been reported to phosphorylate Cx43 to down-regulate Cx43 GJIC in response to active Src in different cell lines (51, 52), we investigated whether Tyk2 also indirectly affects serine phosphorylation. Cx43 serine phosphorylation levels were evaluated using phosphoserine-specific antibodies to pSer-279/pSer-282 (MAPK target) and pSer-368 (PKC target). pSer-279/pSer-282 and pSer-368 levels were up-regulated in the presence of active Tyk2. Finally, although the amount of Cx43 at the plasma membrane decreased (Fig. 3A), active Tyk2 directly or indirectly caused an overall increase in the total amount of Cx43. Numerous studies have shown that

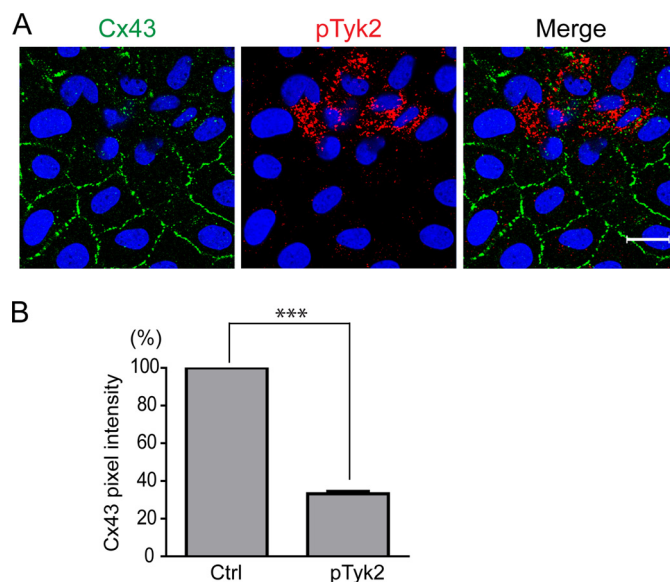


**FIGURE 3. Effect of Tyk2 on the cellular localization of Cx43.** *A*, cellular localization of endogenous Cx43 and constitutively active Tyk2 (Tyk2<sub>V678F</sub>) in NRK cells detected by immunofluorescence (green, Cx43; blue, DAPI-stained DNA; red, active Tyk2). Scale bar is 20  $\mu$ m. *B*, quantification of Cx43 expression level at the plasma membrane. Cx43 pixel intensity of 204 cell pairs containing p-Tyk2 was normalized to the Cx43 pixel intensity of 204 cell pairs without p-Tyk2 (*Ctrl*) by ImageJ software. Cell pairs with or without p-Tyk2 were from the same images. The data are representative of three independent experiments (\*\*\*,  $p < 0.001$ ).

differentially phosphorylated Cx43 results in multiple electrophoretic isoforms: a fast migrating isoform (P0) and multiple slower migrating isoforms (P1 and P2) (2, 53, 54). In particular,



## Tyk2 Phosphorylates Cx43

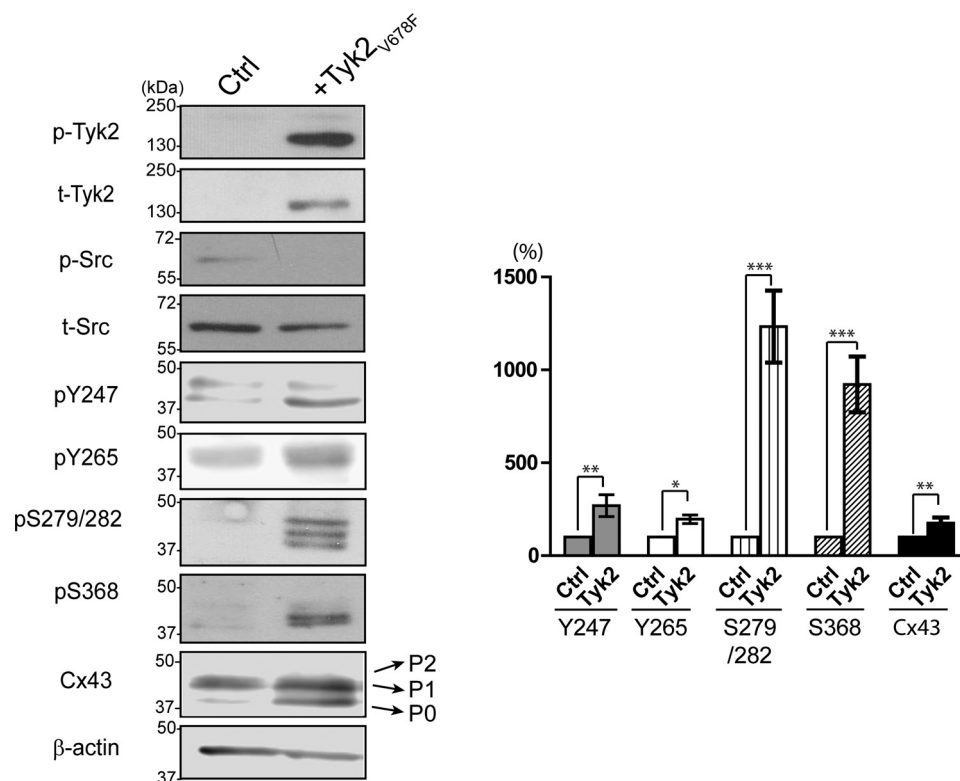


**FIGURE 4. Phosphorylation of Cx43 by Tyk2 in NRK cells.** Western blotting of active Tyk2 (p-Tyk2), total Tyk2, active Src (p-Src), total Src, Cx43 pTyr-247, pTyr-265, pSer-279/pSer-282, pSer-368, and total Cx43 from NRK cells without (Ctrl, control) or with transfection of Tyk2<sub>v678F</sub>. The Cx43 mobility shifts (P0, P1, and P2) are labeled. Relative protein levels were quantified by analyzing the scanned blots using ImageJ software with normalization of protein expression to the control lane (value set arbitrarily as 100%). The data are representative of three independent experiments (\*,  $p < 0.05$ ; \*\*,  $p < 0.01$ ; \*\*\*,  $p < 0.001$ ).

the P2 isoform has been found at the stage of gap junctional plaques. Consistently, Western blotting analysis (here and next sections) showed an increase in the lower migrating P0 and P1 isoforms of Cx43 in the presence of active Tyk2.

Cx43 gap junction channels are localized in detergent-insoluble junctional plaques (55, 56). To confirm that the increased amount of Cx43 does not lead to an increase in the amount of Cx43 at junctional plaques, we assessed the level of Triton X-100 detergent solubility. The detergent extraction Western blotting data show that active Tyk2 in NRK cells decreased the detergent-insoluble fraction of Cx43 (Fig. 5A). Quantification of the data revealed that the control insoluble to insoluble + soluble ratio ( $I/(S + I)$ ) was  $67.1 \pm 6.0\%$ . However, the number of assembled gap junctions significantly decreased to  $19.5 \pm 0.9\%$  in the presence of active Tyk2. The decreased amount of Cx43 in junctional plaques was corroborated by a biotinylation assay, which detected a significant decrease in the amount of Cx43 at the plasma membrane (Fig. 5B).

*Interplay between Src and Tyk2 in the Regulation of Cx43*—Murakami *et al.* (61) observed that v-Src-transfected cells indirectly cause constitutive activation of Tyk2 and STAT3. Therefore, a modified NRK cell line containing a temperature-sensitive v-Src (called LA-25), commonly used in the gap junction field to characterize Cx43 regulation by v-Src (51, 57), was used to study the effect of Tyk2 on Cx43 tyrosine phosphorylation levels upon Src activation. v-Src is active in this cell line at the permissive temperature (35 °C) and not at the non-permissive temperature (40 °C). Of note, temperature alone does not affect gap junction communication in NRK or LA-25 cells (58),

and Tyk2 is endogenously expressed in LA-25 cells. Initially, Western blotting data confirmed that active v-Src at 35 °C resulted in the activation of endogenous Tyk2 (Fig. 6A). Immunostaining data then indicated that after 4 h of v-Src activation, endogenous Tyk2 colocalized with Cx43 at the plasma membrane (Fig. 6B). After 12 h, there was a decrease in the level of Cx43 and Tyk2 colocalization as well as the amount of Cx43 at the plasma membrane. These results are similar to the overexpression of active Tyk2 in the NRK cells (Fig. 3). Next, Tyk2 siRNA was transfected into the LA-25 cells (35 °C) to differentiate the effect of v-Src and Tyk2 on direct and indirect phosphorylation of Cx43 (Fig. 7). Tyk2 siRNA significantly reduced the level of active Tyk2 (>75%). Equally important, the Tyk2 siRNA did not affect the level of active v-Src. Knockdown of Tyk2 in the presence of active v-Src significantly decreased the level of Tyr-247 and Tyr-265 phosphorylation as compared with control (scramble siRNA). Indirect serine phosphorylation was also affected by the knockdown of Tyk2. Although pSer-279/pSer-282 phosphorylation was reduced by ~50%, phosphorylation of pSer-368 was reduced by almost ~75% in the absence of Tyk2. Finally, the knockdown of Tyk2 led to a decrease in the total level of Cx43. Altogether, the data indicate that similarities exist in the residues affected by Src or Tyk2, but differences exist in the level of phosphorylation at each site and the overall amount of protein.

*Tyk2 Increases Total Cx43 Protein Level through the STAT3 Pathway*—In both the NRK and LA-25 cells, active Tyk2 caused an increase in the total protein level of Cx43. To determine the mechanism for this effect, cycloheximide was used to compare

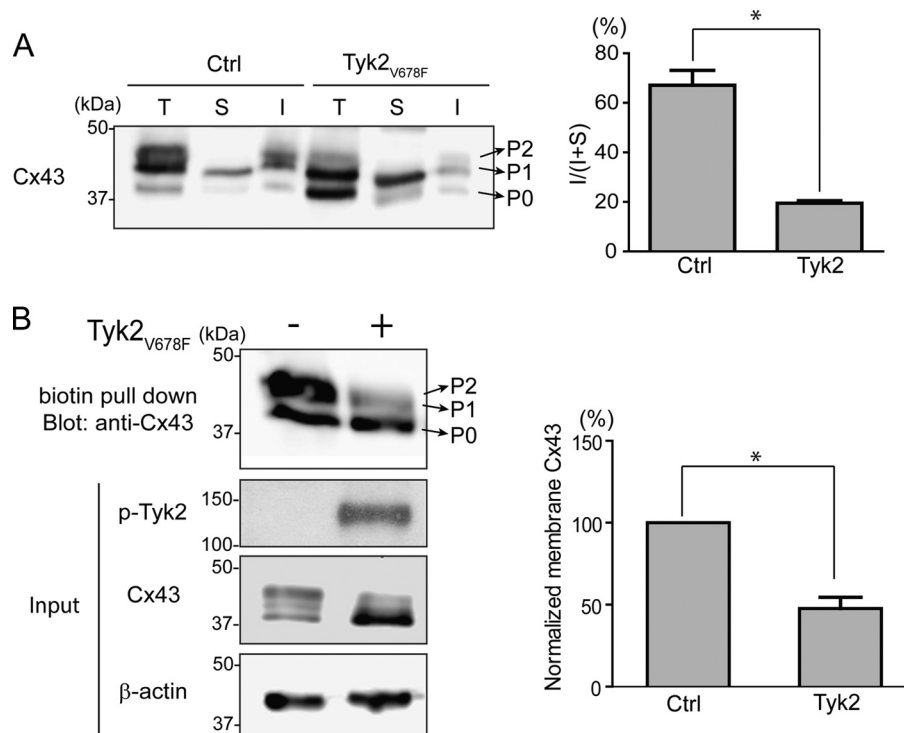


**FIGURE 5. Effect of Tyk2 on the plasma membrane localization of Cx43 in NRK cells.** *A*, Triton X-100 solubility assay. Equal amounts of total protein fraction (*T*), Triton X-100-soluble fraction (*S*), and the insoluble fraction (*I*) were run on SDS-PAGE and blotted with anti-Cx43 antibody. Protein levels were quantified to determine the insoluble to insoluble + soluble ratio [ $I/(I + S)$ ] ( $^*p < 0.05$ ). *B*, biotinylation assay. NRK cells with or without Tyk2<sub>V678F</sub> transfection were cell surface-biotinylated. Biotinylated proteins were pulled down by immobilization on streptavidin-agarose beads and immunoblotted for Cx43. Protein levels of biotinylated Cx43 were quantified ( $^*p < 0.05$ ). Input shows active Tyk2 and Cx43 protein in the cell lysate. *Ctrl*, control.

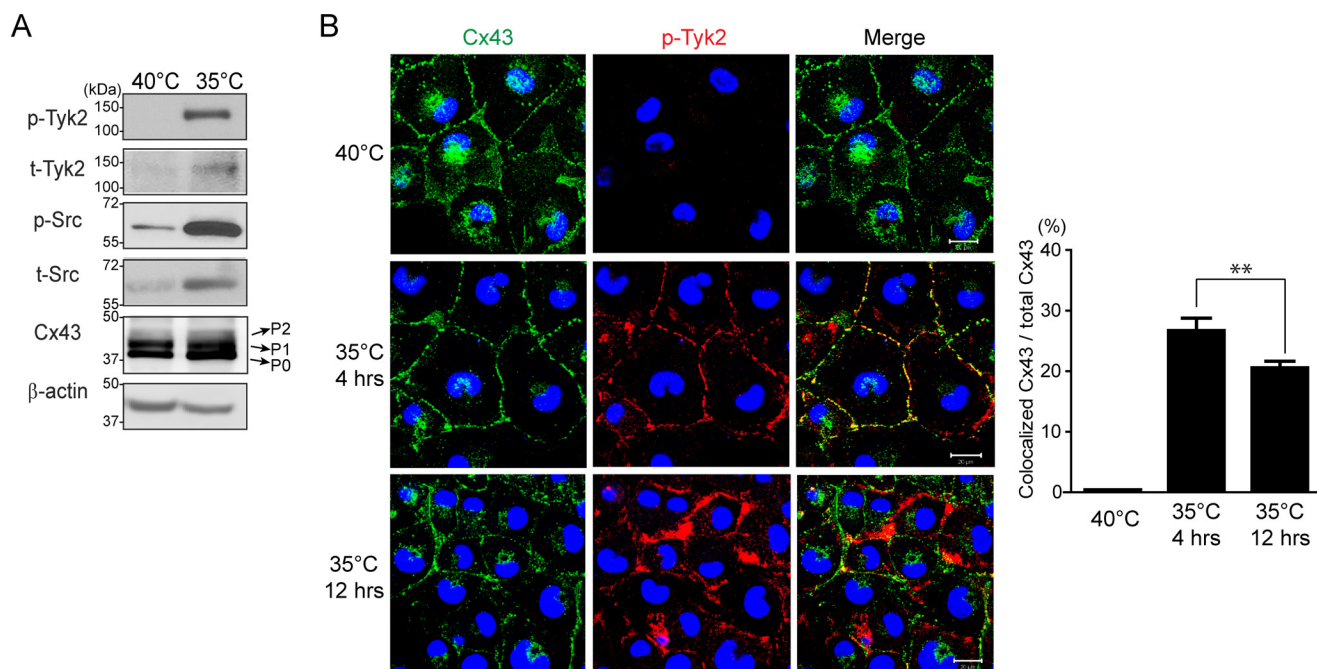


**FIGURE 6. Colocalization of endogenous Tyk2 and Cx43 in LA-25 cells.** *A*, Western blotting of active Tyk2 (p-Tyk2), total Tyk2, Src (p-Src), total Src and Cx43 in LA-25 cells at 40 and 35 °C. *B*, cellular localization of endogenous Cx43 and active Tyk2 in LA-25 cells at 40 °C or 35 °C was visualized by using immunofluorescence (green, Cx43; blue, DAPI-stained DNA; red, Tyk2). Scale bar is 20 μm. Colocalization of Cx43 and p-Tyk2 was analyzed based on 12 images from three independent experiments. The Manders method was used to measure the green signal (Cx43) coincident with the red signal (active Tyk2) over the total intensity of green signal ( $^{**}p < 0.01$ ).

the turnover rate of Cx43 with or without Tyk2 (Fig. 8). Western blotting analysis of Cx43 from NRK cells revealed that active Tyk2 increased the Cx43 turnover. The data suggest that

the increased protein level of Cx43 is not a result of direct tyrosine or indirect serine phosphorylation. Next, RT-PCR from the cell lysate of NRK cells transfected with active Tyk2 was used to

## Tyk2 Phosphorylates Cx43

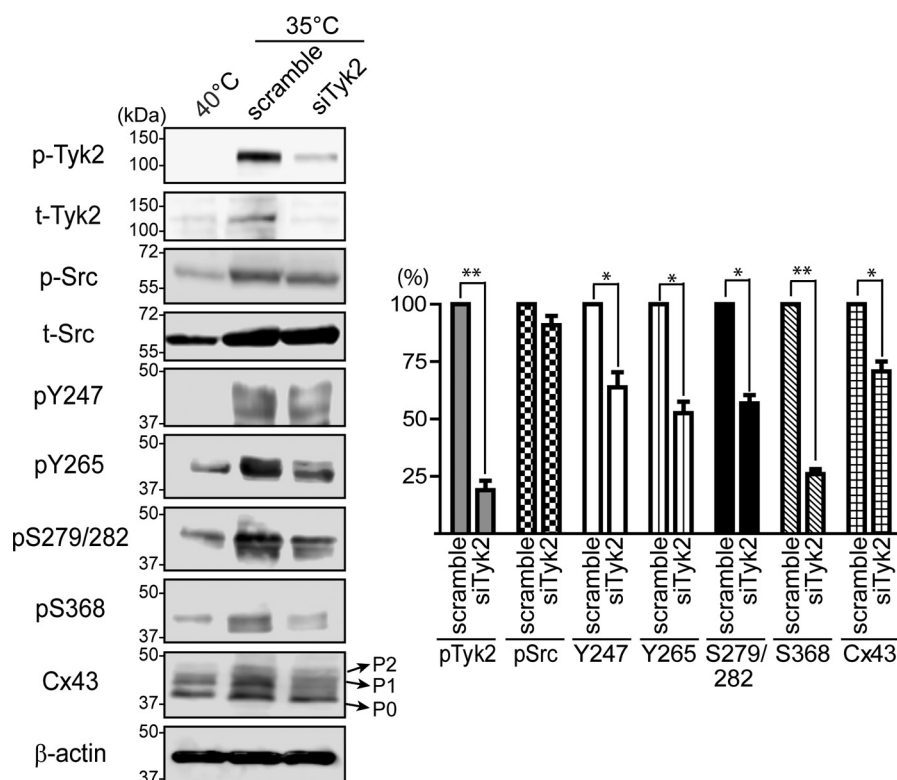


**FIGURE 7. Effect of Tyk2 knockdown on the phosphorylation level of Cx43 in LA-25 cells.** Western blotting of active Tyk2 (p-Tyk2), total Tyk2, active Src (p-Src), total Src, Cx43 pTyr-247, pTyr-265, pSer-279/pSer-282, pSer-368, and total Cx43 from LA-25 cells at 40 or 35 °C treated with scrambled or Tyk2 siRNA for 12 h. Relative protein levels were quantified using ImageJ software and normalized to the expression level in the scramble RNA-treated sample at 35 °C (\*,  $p < 0.05$ ; \*\*,  $p < 0.01$ ).

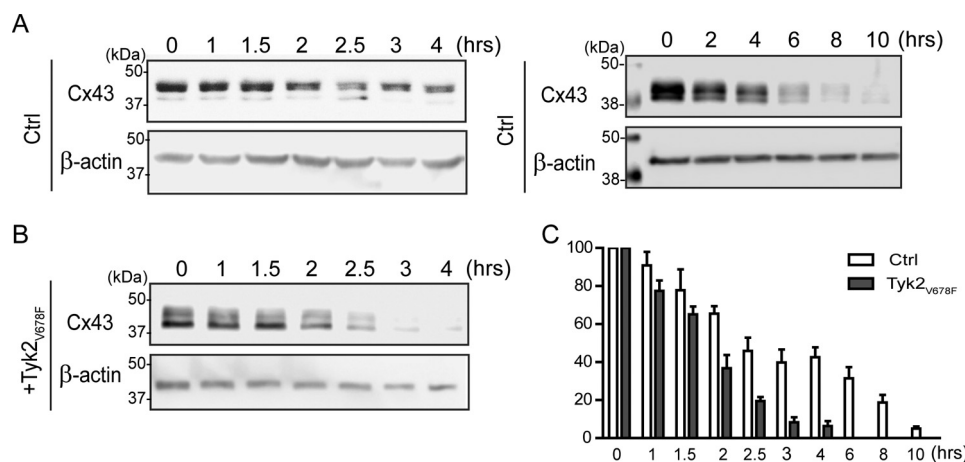


**FIGURE 8. Effect of Tyk2 on the turnover rate of Cx43 in NRK cells.** Control (A, *Ctrl*) or transfected NRK cells (B) with the constitutively active Tyk2 (Tyk2<sub>v678F</sub>) construct were treated with 100 μg/ml cycloheximide for different durations prior to lysis. Total Cx43 protein was immunoblotted. C, the protein level of three independent experiments was quantified using ImageJ software and normalized to the protein level at 0 h.

determine if active Tyk2 indirectly affects the level of Cx43 mRNA. Using different numbers of RT-PCR cycles, the data revealed that active Tyk2 caused an increase in the level of Cx43 mRNA (Fig. 9A). Actin was used as a loading control. Because Tyk2 activates the STAT signaling pathway, we tested whether this is the mechanism that leads to increased mRNA and protein levels. Experiments performed using NRK cells incubated with the STAT1/3/5 inhibitor nifuroxazide or the STAT3/5 inhibitor SH-4-54 eliminated the effect of active Tyk2 increasing Cx43 mRNA (Fig. 9B) and protein levels (Fig. 10A). Based upon NRK cells expressing a very small amount of STAT1 and

no STAT5 (Fig. 10B), the data strongly indicate that Tyk2 activation of STAT3 is responsible for the increased Cx43 mRNA and subsequent increased protein levels.

*Tyk2 Mediates Ang II Regulation of Cx43*—Dysregulation of RAS affects many aspects of the cardiovascular system (35, 36, 47, 48). RAS activation also decreases Cx43 GJIC and changes cellular localization (43, 44). Based upon the involvement of Tyk2 in RAS signaling via angiotensin II receptor 1, we tested whether the changes observed for Cx43 were caused by Tyk2. Western blotting analysis was used to investigate wild-type (WT) Tyk2-transfected NRK cells treated with Ang II (Fig. 11).

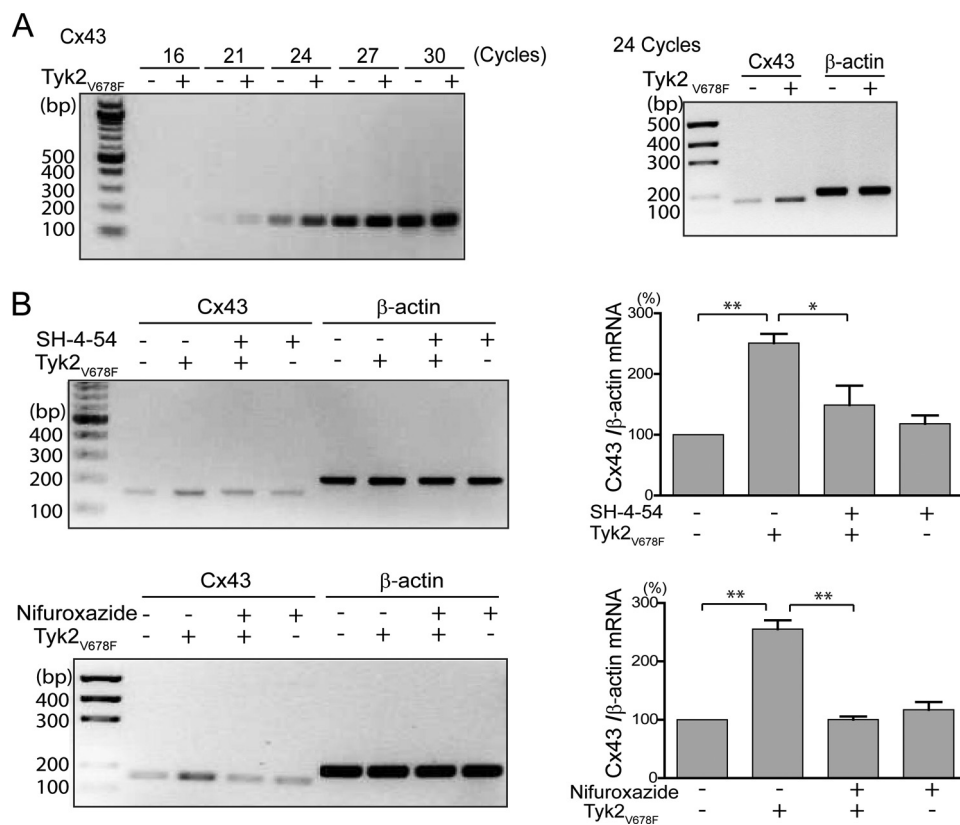


**FIGURE 9. Effect of STAT3 activation by Tyk2 on Cx43 mRNA level.** *A*, RT-PCR shows Cx43 mRNA level with or without transfection of active Tyk2 (Tyk2<sub>V678F</sub>). The appropriate number of cycles was determined by testing different number of cycles (16, 21, 24, 27, and 30 cycles) for Cx43 amplification (top panel). Cx43 intensity increased up to 24 cycles, where a plateau was reached; thus 24 cycles were used to run semiquantitative RT-PCR. Cx43 and β-actin were amplified for 24 cycles and ran on 2% agarose gel (right panel). *B*, NRK cells with or without active Tyk2 (Tyk2<sub>V678F</sub>) transfection for 8 h were treated with the STAT3/5 inhibitor SH-4-54 (5 μM) or the STAT1/3/5 inhibitor nifuroxazide (50 μM) for another 16 h. Cx43 and β-actin were amplified for 24 cycles and run on 2% agarose gel. Cx43 and β-actin mRNA levels were quantified by densitometry from three independent experiments (\*, *p* < 0.05; \*\*, *p* < 0.01).

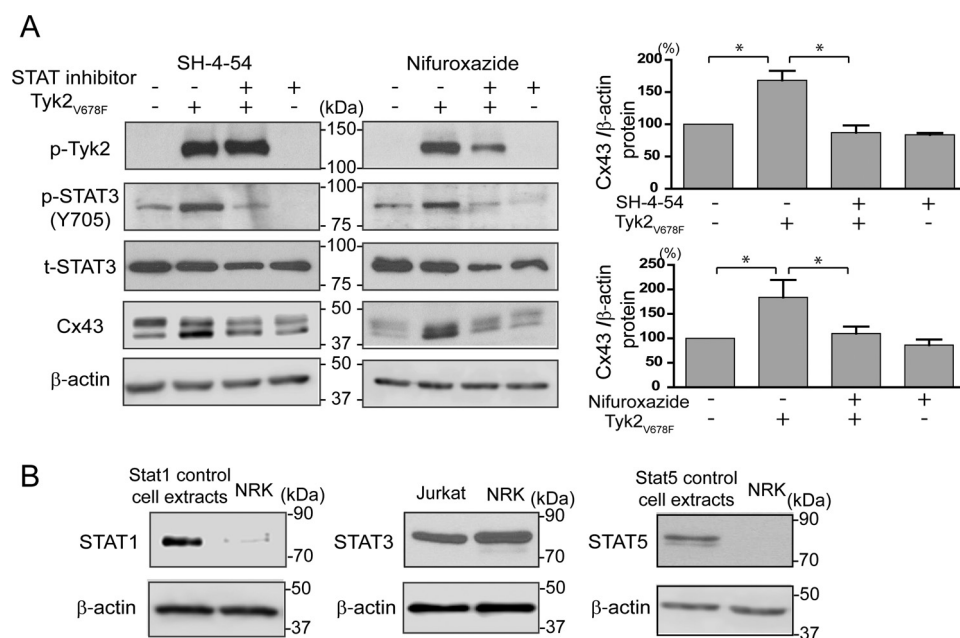


**FIGURE 10. Effect of STAT3 activation by Tyk2 on Cx43 protein level.** *A*, Western blotting analysis of active Tyk2 (p-Tyk2), active STAT3 (p-STAT3), total STAT3, and Cx43 in NRK cells transfected with or without active Tyk2 (Tyk2<sub>V678F</sub>) and treated with and without SH-4-54 or nifuroxazide. Cx43 protein level was quantified using ImageJ software (\*, *p* < 0.05). *B*, Western blotting analysis of STAT1, STAT3, and STAT5 from NRK cell lysate. Cell extracts from HeLa cells treated with IFN-α (100 ng/ml) for 5 min were used as a positive control for blotting STAT1 and STAT5. Jurkat cell lysate was used as the positive control for blotting STAT3.



## Tyk2 Phosphorylates Cx43

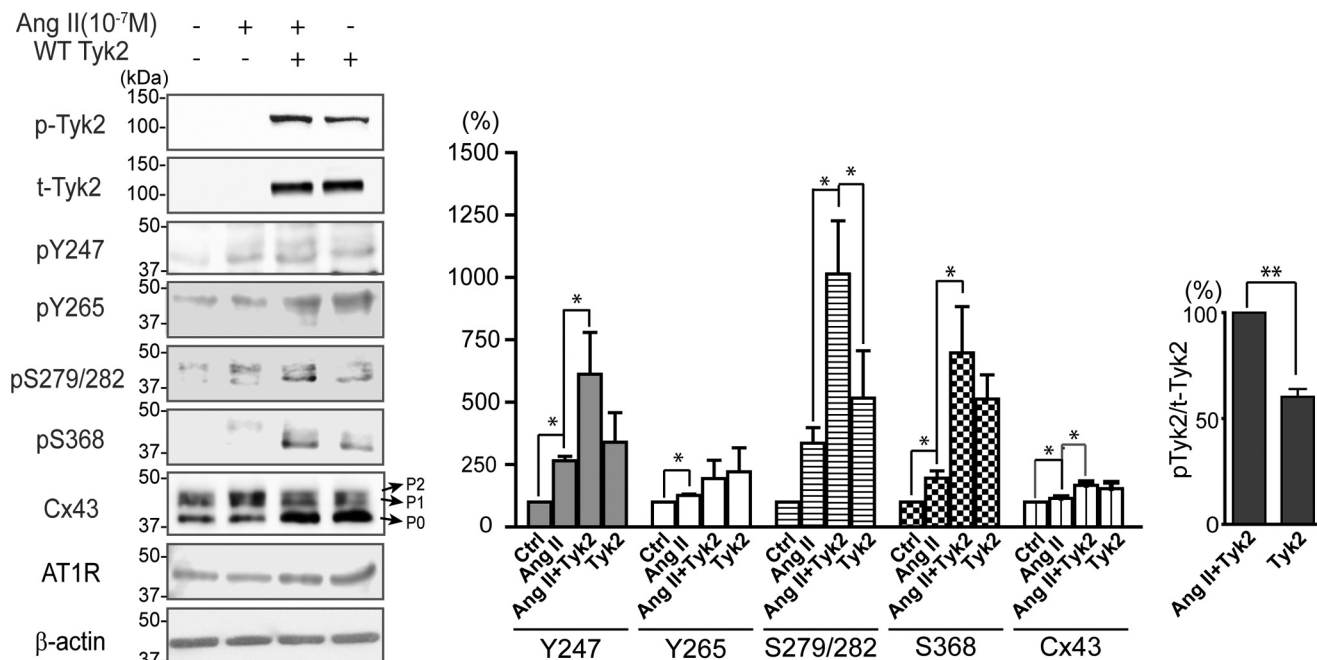


FIGURE 11. **Effect of Ang II activation of Tyk2 on the phosphorylation level of Cx43.** Western blotting analysis of active Tyk2 (p-Tyk2), total Tyk2, pTyr-247, Cx43 pTyr-265, pSer-279/pSer-282, pSer-368, total Cx43, and the angiotensin II type 1 receptor (AT1R) from NRK cells with or without transfected WT Tyk2 and treated with or without Ang II ( $10^{-7}$  M). The protein phosphorylation levels were quantified using ImageJ software (\*,  $p < 0.05$ ; \*\*,  $p < 0.01$ ).

The transfection of WT Tyk2 alone caused a basal level of activation; however, the presence of Ang II significantly increased the amount of active Tyk2. The presence of Tyk2 or Ang II alone caused a significant increase in the level of Tyr-247, Tyr-265, Ser-279/Ser-282, and Ser-368 phosphorylation. Although the phosphorylation levels of Tyr-247, Ser-279/Ser-282, and Ser-368 were highest in the presence of both Tyk2 and Ang II, only Ser-279/Ser-282 phosphorylation was statistically significant compared with Tyk2 alone. Interestingly, although the presence of Tyk2 or Ang II alone caused an increase in the level of total Cx43, which was further increased in the company of both, the presence of Tyk2 but not Ang II caused an increase in the lower migrating P0 and P1 isoforms of Cx43.

**Phosphorylation of Cx43 Residue Tyr-247 Prevents the Binding of Tubulin**—Previous studies have identified that Cx43 phosphorylation can inhibit the interaction with the ZO-1 PDZ-2 domain (pSer-373 (9)) or enhance the interaction with the Nedd4 WW2 domain (pSer-279/pSer-282 (12)). Additionally, a Cx43 phosphopeptide (pTyr-247) was not able to interact with purified tubulin *in vitro* (8). Because the pTyr-247 level was significantly increased by Tyk2 in the cells (Figs. 4 and 11), a biotin-tagged Cx43 pTyr-247-phosphorylated peptide or non-phosphorylated (Lys-234–Ser-255) version was used in a pull-down assay to assess the interaction with  $\beta$ -tubulin in NRK cell lysate (Fig. 12). The data indicate that Tyk2 phosphorylation of Tyr-247 would inhibit the interaction with  $\beta$ -tubulin.

## Discussion

Up until now, Src has been the only non-receptor tyrosine kinase to directly phosphorylate Cx43 leading to an inhibition of GJIC and subsequent gap junction disassembly (59, 60). In this study, we identified another tyrosine kinase, Tyk2, which can directly phosphorylate Cx43 on residues Tyr-247 and Tyr-

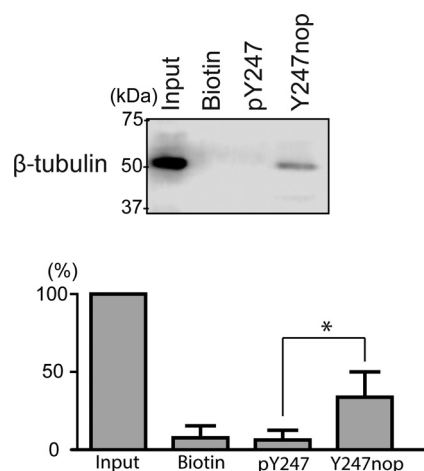


FIGURE 12. **Effect of Cx43 Tyr-247 phosphorylation on the interaction with  $\beta$ -tubulin.** Western blotting analysis of  $\beta$ -tubulin from a biotin pull-down assay using a biotinylated-phosphopeptide, Cx43CT-(234–255) (pY247) or non-phosphopeptide (Y247nop) bound to streptavidin beads and incubated with NRK cell lysate. Biotin bound to streptavidin-agarose beads was used as the negative control. Protein levels were quantified using ImageJ (\*,  $p < 0.05$ ) and normalized by input (1:20 loaded compared with pull-down groups) from three independent experiments.

265 and lead to indirect phosphorylation on residues Ser-368 and Ser-279/Ser-282. Although this phosphorylation pattern is similar to what has been observed following Src activation (51), importantly, the response caused by Tyk2 (*e.g.* overexpression of the constitutively active version) occurred when Src was inactive in NRK cells. This indicates that different signaling pathways can lead to the same regulation of Cx43 gap junctions. Unexpectedly, when v-Src was activated in the LA-25 cells at the permissive temperature, Tyk2 was activated as well. This observation is not unique to the LA-25 cells, as constitutive activation of Tyk2 has been observed in a human gallbladder



adenocarcinoma cell line transfected with v-Src (61). A significant decrease in the phosphorylation of Cx43 residues Tyr-247, Tyr-265, and Ser-279/Ser-282, and especially Ser-368 (75% decrease), was observed in the LA-25 cells at the permissive temperature when the expression of Tyk2 was knocked down. The data suggest that although activation of Tyk2 and v-Src lead to phosphorylation of the same Cx43CT residues, they are not identical in level at each site. Additionally, the data would suggest that activation of both Tyk2 and v-Src works together to amplify the phosphorylation response on Cx43. Differences in the level of phosphorylation between Tyk2 and Src can be explained from the knowledge that the Tyk2 SH2 domain does not need a phosphate to interact with its substrate, combined with the absence of an SH3 domain (62).

A consistent observation from the immunofluorescence experiments was that prolonged activation of Tyk2 led to a near complete removal of Cx43 from the plasma membrane. Saidi Brikci-Nigassa *et al.* (8) showed that a Cx43CT phosphopeptide (pTyr-247) does not interact with purified tubulin. We used a biotinylated Cx43CT control (Lys-234–Ser-255) and phosphopeptide (pTyr-247) in a pull-down assay using NRK cell lysate to show that phosphorylation inhibits the Cx43CT/ $\beta$ -tubulin interaction. Increased levels of pTyr-247 by Tyk2 (or Src) would block the Cx43 interaction with tubulin (8). At the gap junction plaque, this may be a mechanism in the disassembly process; at the trans-Golgi network, this may reroute trafficking to the plasma membrane (*e.g.* lateral membrane *versus* intercalated disc) or inhibit trafficking to the plasma membrane, leading to increased intracellular proteasomal and/or lysosomal degradation (63). Other mechanisms that would contribute to the lack of Cx43 at the plasma membrane include phosphorylation of residues Ser-279/Ser-282 (MAPK) and Ser-368 (PKC). Phosphorylation of Ser-279/Ser-282 increases the binding affinity by 2-fold for the WW2 domain from the ubiquitin ligase Nedd4, leading to Cx43 gap junction degradation (12, 13, 64). Activation of PKC can halt the assembly of new gap junctions, and phosphorylation on Ser-368 has been implicated in affecting gating and/or disassembly (65–67). Of note, although not investigated in this study, Src activation also leads to phosphorylation of Cx43 on Ser-373 by Akt (68). The importance of phosphorylation on this site is that the interaction with ZO-1 is inhibited, transitioning Cx43 from the non-junctional plasma membrane into the gap junction plaque and then through the degradation pathway(s). Less clear is the functional role of phosphorylation on Tyr-265. One possibility is that the Src SH3 domain interaction with Cx43 residues Ala-276–Pro-280 positions the Src kinase domain to phosphorylate Tyr-265, forming a SH2 binding domain (45). The next step would be for the Src SH2 binding domain to interact with pTyr-265 and place the Src kinase domain within distance to phosphorylate Tyr-247. This potential mechanism would explain why pTyr-265 appears here and in other studies to label a larger population of plaques than pTyr-247 (51). Another function of Tyr-265 is to form part of a tyrosine-based sorting motif (YXX $\Phi$ , where Y is tyrosine, X is any amino acid, and  $\Phi$  is a bulky hydrophobic amino acid), which enables an interaction with the  $\mu$  subunit of the heterotetrameric adaptor protein complex AP-2 to mediate clathrin-dependent internalization of Cx43. However, the abil-

ity of this tyrosine residue to bind AP2 is negatively influenced by tyrosine phosphorylation. For example, phosphorylation of GluN2B residue Tyr-1472 within the YEKL tyrosine-based sorting signal motif by Fyn inhibits AP2 binding and the internalization of GluN2B-containing NMDA-type glutamate receptors (69). Similarly, phosphorylation of GluN2A by Src inhibits endocytosis of GluN2A-containing NMDA-type glutamate receptors (70, 71).

One difference observed in our studies, and those of others, performed *in vitro* as compared with *in vivo* is the effect of Ang II on Cx43 protein level. We identified that activation of Tyk2 by Ang II *in vitro* causes an increase in Cx43 protein level via the STAT3 pathway. Other *in vitro* examples of an increase in Cx43 protein level include exposing freshly isolated aortas of wild-type mice to Ang II for 4 h and the aorta smooth muscle cell line A7r5 to Ang II from 2 to 48 h (maximum expression was observed at 4 h and was maintained to the last time point of 48 h) (72, 73). Conversely, chronic exposure of Ang II in animal models shows a decrease in the protein level of Cx43. This was seen in the atria and ventricles of the transgenic mouse model of cardiac-restricted overexpression of ACE (ACE8/8) described above (40) and in the double transgenic rat, which harbors the human renin and angiotensinogen genes (dTGR) (74). Although the length of Ang II exposure (acute *versus* chronic) and experimental conditions (*in vitro* and *in vivo*) are important factors when interpreting the protein level of Cx43, the combined data can be explained from the study of Kostin *et al.* (75). Cx43 expression was increased in the compensated hypertrophic stage from the left ventricles of pressure-overloaded human hearts with valvular aortic stenosis but decreased and heterogeneously distributed throughout the ventricles in the decompensated stage (75).

We identified that the effect Tyk2 elicited on the Cx43 protein level in NRK cells was mediated through the activation of STAT3. However, this increase did not correlate with increased GJIC, as Cx43 was not localized to the plasma membrane. Evidence that STAT3 directly increases the transcriptional activity of Cx43 was provided by Ozog *et al.* (76). Three putative ciliary neurotrophic factor-response elements (binding sites for STAT3 dimers that contain base sequences TTCCN3–5AA) were identified in the promoter region of the mouse Cx43 gene (located at regions –1510, –1179, and –893) as essential for enhanced Cx43 expression. Interestingly, STAT3 activation also leads to down-regulation of E-cadherin (77). One mechanism for the decreased gap junction assembly may be explained by the observation that expression of E-cadherin is necessary to enable the assembly of Cx43 into gap junctions (78).

In conclusion, the phosphorylation of Cx43 at different sites controls gap junction assembly, size, gating, and turnover. Our understanding of these mechanisms has been aided by the identification of the kinases involved and the exact location of their phosphorylation on the Cx43CT domain. Through the use of MS and phospho-specific antibodies, patterns of phosphorylation have been correlated with different cellular conditions (51, 79). For example, Solan and Lampe (6) put forth the notion that differential coordination of kinase activation and Cx43 phosphorylation control the specific routes of disassembly. Their

## Tyk2 Phosphorylates Cx43

model describes the interplay between CK1, PKA, Akt, MAPK, PKC, and Src, each of which phosphorylates a distinct set of Cx43 residues. Here we identified that more than one kinase can directly phosphorylate the same Cx43CT residues. In addition, Tyk2 and Src alone caused a differential level of phosphorylation at each residue (directly or indirectly), with the maximum level detected when both were active. These data suggest an additional layer of complexity that may need to be considered when describing the full impact of phosphorylation on Cx43 regulation. Future studies need to examine whether Tyk2 and Src always work together to decrease Cx43 gap junction communication; and if not, what are the cellular conditions in which they work independently, and does this differentially affect gap junction communication?

### Experimental Procedures

**Cell Culture**—NRK and LA-25 cells (NRK cells contain temperature-sensitive  $v$ -Src) were generous gifts from Dr. Paul Lampe (Fred Hutchinson Cancer Research Center). The MDA-MB-231 cell line was from Dr. Melissa Teoh-Fitzgerald (University of Nebraska Medical Center). All cells were grown in Dulbecco's modified Eagle's medium (DMEM) (Hyclone, Thermo Fisher Scientific Inc.) supplemented with 10% fetal bovine serum (FBS) (Hyclone, Thermo Fisher Scientific Inc.) and antibiotics in an atmosphere of humidified 5% CO<sub>2</sub>.

**Antibody and Immunostaining**—The following antibodies were used in this study: Cx43 monoclonal antibodies against amino acids 360–382 (Cx43CT1 and Cx43IF1, as described (80, 81)); Cx43 polyclonal antibody (C6219, Sigma-Aldrich); anti-Cx43-phosphorylated Tyr-247, anti-phosphorylated Tyr-265, and anti-phosphorylated Ser-279/Ser-282 (51) (all generous gifts from Dr. Paul Lampe, Fred Hutchinson Cancer Research Center); anti-Cx43-phosphorylated Ser-368 (Millipore); non-specific phosphotyrosine antibody (pTyr-100, Cell Signaling Technology); anti-Tyk2 (Santa Cruz Biotechnology) and anti-active Tyk2 (phosphorylated 1054/1055); anti-tubulin  $\beta$  (Sigma); antibodies against total and active Src (phosphorylated Tyr-416, Millipore); and STAT antibodies sampler kit (catalog number 9939, Cell Signaling Technology).

Cells were immunostained as described previously (82). Briefly, cells grown on coverslips to ~60% confluence were fixed with 3.7% paraformaldehyde for 10 min. Cells were blocked for 30 min at room temperature by MPS buffer (1 $\times$  PBS, 1% goat serum) containing 0.2% Triton X-100 for permeabilization. Then, cells were immunostained with the appropriate primary antibodies at room temperature for 1 h followed by several PBS-0.5% Tween washes. Secondary antibodies (Alexa 594-conjugated goat anti-rabbit antibody and/or Alexa 488-conjugated goat anti-mouse antibody) were applied for 1 h at room temperature. Images of immunostained cells were acquired with a Zeiss 510 Meta confocal laser-scanning microscope using a 63 $\times$  1.4 numerical aperture objective with appropriate filters. Colocalization was quantified using the Manders method in ImageJ (83).

**In Vitro Kinase Assay**—Rat Cx43CT-(236–382) was expressed and purified as described previously (84). An *in vitro* kinase screen was performed by Eurofins Scientific using the purified protein. The catalytic domain of JAK1 (residues 866–

1154), JAK2 (residues 808–1132), and Tyk2 (residues 875–1187) were used to phosphorylate the Cx43CT. A positive control was used for each kinase (JAK1, GEEPLYWSFPAKKK; JAK2, KTFCTGPEYLAPEVRRERPRILSEEEQEMFRDFY-IADWC; and Tyk2, GGMEDIYFEFMGGKKK). Controls and Cx43CT were incubated with the tyrosine kinase and [ $\gamma$ -<sup>33</sup>P]ATP for 40 min at 30 °C and then transferred to P30 Filtermat for substrate capture. Assays were performed in duplicate, and acid blanks were used as a negative control. The level of phosphorylation for each sample was determined using a Merck Millipore radiometric assay.

**Mass Spectrometry**—Purified rat Cx43CT<sup>236–382</sup> (12.5 nmol) was incubated with 1.5  $\mu$ g of Tyk2 (amino acids 833–1187, ThermoFisher Scientific) and 500  $\mu$ M ATP at 30 °C for 15 h. In the control group, the volume of Tyk2 was substituted by reaction buffer (25 mM HEPES (pH 7.5), 10 mM MgCl<sub>2</sub>, 0.5 mM EGTA, and 0.005% Brij-35). The reaction was stopped on ice, and 1 nmol of protein was run on an SDS-PAGE and Western-blotted using a phosphotyrosine antibody. 10 nmol of protein was run on an SDS-PAGE and stained with Coomassie. The Cx43CT band was cut and sent to the Beth Israel Deaconess Medical Center mass spectrometry facility for analysis (85).

**GST Pulldown Assay**—The GST pulldown assay was modified from (13). Briefly, purified GST-Cx43CT fusion and GST control proteins were bound to glutathione-Sepharose beads in buffer containing 25 mM Tris-HCl (pH 7.4), 150 mM NaCl, 1 mM DTT, 0.5% Triton X-100, and Complete protease inhibitor (Roche). 4 mg of MDA-MB-231 or LA-25 cell lysate protein (in cell lysis buffer containing 25 mM Tris-HCl (pH 7.4), 150 mM NaCl, 0.5% Triton X-100, 0.5% sodium deoxycholate, 2 mM EDTA, PhosSTOP (Roche), and Complete protease inhibitor) was incubated with GST-Cx43CT fusion or the GST control for 6 h at 4 °C on a rotating wheel. Beads were washed five times with cell lysis buffer, and the bound proteins were eluted with SDS-PAGE sample buffer and analyzed by Western blotting analysis.

**Co-immunoprecipitation**—NRK or LA-25 cells were lysed in Complete lysis buffer (50 mM Tris-HCl (pH 7.4), 150 mM NaCl, 0.5% sodium deoxycholate, 0.5% Triton X-100, 5 mM NaF, and Complete protease inhibitor), maintained on ice for 30 min, precleared with protein G beads for 30 min at 4 °C, and then spun at 12,000 rpm for 15 min. Total protein was assessed using the bicinchoninic acid (BCA) protein assay kit (Pierce). 2 mg of lysate was incubated with 2  $\mu$ g of Cx43 polyclonal or rabbit IgG (4 h at 4 °C) and then incubated with 100  $\mu$ l of protein G-Sepharose (GE Healthcare) overnight at 4 °C. The Sepharose was washed four times with cold lysis buffer, and the co-immunoprecipitation product was analyzed by SDS-PAGE and Western blotting analysis.

When detecting the tyrosine phosphorylation levels, 5 mM Na<sub>3</sub>VO<sub>4</sub> was added in the blocking and primary antibody buffer to minimize the loss of phosphorylation. Western blotting data were scanned and quantified using ImageJ software as described elsewhere (86).

**Tyk2 siRNA Treatment**—Tyk2 siRNA (Invitrogen) was used to knock down Tyk2 expression in LA-25 cells. Oligonucleotide from the non-target pool (Dharmacon) was used as the negative control. Lipofectmine RNAiMAX (Invitrogen) was used to

carry the oligonucleotide according to manufacturer's protocol. Cells were treated with Tyk2 siRNA for 36 h and then incubated at 35 °C for another 12 h. Protein levels were detected by Western blotting analysis.

**Cycloheximide Treatment and Cx43 Degradation**—Cells seeded equally on 60-mm dishes were grown for 24 h to 70–80% confluency before transfection. 24 h post-transfection, cells were treated with 100 µg/ml cycloheximide (Cell Signaling Technology) for up to 10 h to inhibit protein synthesis. Cells were then scraped off at each time point and lysed for Cx43 immunoblotting.  $\beta$ -Actin was also blotted for quantification.

**Triton X-100 Solubility**—The Triton X-100 solubility assay was modified from the method described by Mitra *et al.* (87). NRK cells grown in 10-cm dishes were rinsed three times with PBS and scraped into 1 ml of lysis buffer (50 mM Tris-HCl (pH 7.4), 1 mM EGTA, 1 mM EDTA, 1 mM PMSF, 100 mM NaCl, PhosSTOP, and Complete protease inhibitor). Then, the cells were sonicated for 10 s on ice. Protein estimation was determined using the BCA method. 450 µl of cell lysate samples was added to 50 µl of 10% SDS, which was saved as total protein, or to 10% Triton X-100 (final concentration of 1%) and incubated at 4 °C for 30 min. Lysates were then separated into cytosolic (supernatant, soluble) and membrane (pellet, insoluble) fractions by centrifugation at 100,000  $\times g$  for 1 h at 4 °C. The pellets were dissolved in 500 µl of dissolving buffer (70 mM Tris-HCl (pH 6.8), 8 M urea, 2.5% SDS, 0.1 M DTT, 5 mM NaF, 5 mM Na<sub>3</sub>VO<sub>4</sub>, and Complete protease inhibitor). Equal volumes of total lysate, Triton X-100, and the soluble and insoluble portions were loaded on a 10% SDS-PAGE and immunoblotted with the Cx43 polyclonal antibody.

**Surface Biotinylation Assay**—Surface biotinylation assay followed the method described by Johnson *et al.* (88). Briefly, cells were seeded in 60-mm dishes in replicate and grown to 70–80% confluence. 24 h after transfection, cells were washed once with PBS, and then 5 ml of ice cold DMEM plus HEPES buffer (pH 7.4, final concentration 30 mM) was added for 10 min at 4 °C. The cells were washed twice with cold PBS-Plus (PBS with 1 mM CaCl<sub>2</sub> and 1 mM MgCl<sub>2</sub>). The biotinylation reaction was performed at 4 °C using freshly prepared EZ-Link Sulfo-NHS-SS-biotin reagent (Pierce) at 0.5 mg/ml in PBS-Plus for 30 min. The reaction was terminated by adding PBS-Plus containing 20 mM glycine. Cells were lysed in lysis buffer (25 mM Tris-HCl (pH 7.5), 0.05% SDS, 20 mM glycine, and Complete protease inhibitor) with homogenization by passage through a 25-gauge needle. 500 µg of total protein was incubated with 100 µl of streptavidin-agarose beads (Pierce) on a rotator overnight at 4 °C. The beads were then washed six times, and the streptavidin-bound biotinylated proteins were eluted and resolved by SDS-PAGE followed by Western blotting analysis.

**Biotin Peptide Pulldown Assay**—Biotin-tagged phosphorylated (Tyr-247) and non-phosphorylated Cx43CT-(234–255) peptides (LifeTein) were bound to streptavidin-agarose resin (GenScript) in PBS. NRK cells were lysed in HEPES lysis buffer (50 mM HEPES, 150 mM NaCl, 0.25% Triton X-100, 2 mM PMSF, 10 mM EDTA, 50 mM NaF, 5 mM Na<sub>3</sub>VO<sub>4</sub>, and PhosSTOP and Complete tablets (pH 7.4)), and total protein concentration was assessed using the BCA protein assay. A total of 2.5 mg of protein lysate was incubated with each of the resin-bound

peptides overnight at 4 °C. Beads were washed three times with PBS before analyzing the pulldown products by SDS-PAGE and Western blotting analysis.

**Semiquantitative RT-PCR**—Semiquantitative RT-PCR was modified from the method described by Marone *et al.* (89). Briefly, NRK cells grown in 35-mm dishes were transfected with Tyk2<sub>V678F</sub> and pretreated with the inhibitor nifuroxazide (50 µM, Millipore) or SH-4-54 (5 µM, Millipore). RNA extractions were carried out with the RNeasy mini kit (Qiagen) according to the manufacturer's protocol. RT was performed with a ProtoScript cDNA synthesis kit (New England Biolabs). The following primers were used: Cx43, 5'-AGCCTCCAAGGAGTT-CCA-3' and 5'-AGAGCACTGACAGCCACA-3'; and  $\beta$ -actin, 5'-CACCCGCGAGTACAACCTTC-3' and 5'-CCCATACC-CACCATCACACC-3'. Cx43 yielded an amplification product of 160 bp and  $\beta$ -actin of 207 bp. DreamTaq Green PCR Master Mix (Thermo Fisher Scientific) was used for PCR amplification. To find out the exponential phase of amplification, different PCR cycles from 16 to 30 were tested. Each set of reaction included a no-sample negative control.

**Statistical Analysis**—All data were analyzed using GraphPad Prism 5.0 and presented as the mean  $\pm$  S.E. A paired *t* test was used to compare differences between the experimental group and control or the two parallel experimental groups. *p* < 0.05 was considered to be statistically significant.

**Author Contributions**—H. L. conducted most of the experiments, analyzed the results, and wrote parts of the manuscript. G. S. and L. Z. performed the biotin peptide pulldown and cycloheximide assays, respectively. G. S. and K. L. S. helped H. L. analyze the mass spectrometry data and edit the manuscript. P. L. S. conceived the idea for the project, analyzed the results, and wrote parts of the manuscript.

**Acknowledgments**—We thank Dr. Paul Lampe (Fred Hutchinson Cancer Research Center, Seattle, WA) for providing the NRK and LA-25 cell lines and antibodies against Cx43 pTyr-265, pTyr-247, pSer-279/pSer-282 and Cx43IF1, and Dr. Melissa Teoh-Fitzgerald (University of Nebraska Medical Center) for providing MDA-MB-231 cells, as well as Dr. Dale W. Laird (Ontario, Canada) for the Cx43-mRFP plasmids.

## References

- Laird, D. W. (2006) Life cycle of connexins in health and disease. *Biochem. J.* **394**, 527–543
- Solan, J. L., and Lampe, P. D. (2005) Connexin phosphorylation as a regulatory event linked to gap junction channel assembly. *Biochim. Biophys. Acta* **1711**, 154–163
- Solan, J. L., and Lampe, P. D. (2007) Key connexin 43 phosphorylation events regulate the gap junction life cycle. *J. Membr. Biol.* **217**, 35–41
- Axelsen, L. N., Calloe, K., Holstein-Rathlou, N. H., and Nielsen, M. S. (2013) Managing the complexity of communication: regulation of gap junctions by post-translational modification. *Front. Pharmacol.* **4**, 130
- Lampe, P. D., and Lau, A. F. (2004) The effects of connexin phosphorylation on gap junctional communication. *Int. J. Biochem. Cell Biol.* **36**, 1171–1186
- Solan, J. L., and Lampe, P. D. (2014) Specific Cx43 phosphorylation events regulate gap junction turnover *in vivo*. *FEBS Lett.* **588**, 1423–1429
- Sosinsky, G. E., Solan, J. L., Gaietta, G. M., Ngan, L., Lee, G. J., Mackey, M. R., and Lampe, P. D. (2007) The C terminus of Connexin43 adopts different conformations in the golgi and gap junction as detected with



- structure-specific antibodies. *Biochem. J.* **408**, 375–385
8. Saidi Brikci-Nigassa, A., Clement, M. J., Ha-Duong, T., Adjadj, E., Ziani, L., Pastre, D., Curmi, P. A., and Savarin, P. (2012) Phosphorylation controls the interaction of the connexin43 C-terminal domain with tubulin and microtubules. *Biochemistry* **51**, 4331–4342
  9. Chen, J., Pan, L., Wei, Z., Zhao, Y., and Zhang, M. (2008) Domain-swapped dimerization of ZO-1 PDZ2 generates specific and regulatory connexin43-binding sites. *EMBO J.* **27**, 2113–2123
  10. Solan, J. L., Marquez-Rosado, L., Sorgen, P. L., Thornton, P. J., Gafken, P. R., and Lampe, P. D. (2007) Phosphorylation at S365 is a gatekeeper event that changes the structure of Cx43 and prevents down-regulation by PKC. *J. Cell Biol.* **179**, 1301–1309
  11. Grosely, R., Kopanic, J. L., Nabors, S., Kieken, F., Spagnol, G., Al-Mugotir, M., Zach, S., and Sorgen, P. L. (2013) Effects of phosphorylation on the structure and backbone dynamics of the intrinsically disordered connexin43 C-terminal domain. *J. Biol. Chem.* **288**, 24857–24870
  12. Spagnol, G., Kieken, F., Kopanic, J. L., Li, H., Zach, S., Stauch, K. L., Grosely, R., and Sorgen, P. L. (2016) Structural studies of the Nedd4 WW domains and their selectivity for the connexin43 (Cx43) carboxyl terminal domain. *J. Biol. Chem.* **291**, 7637–7650
  13. Leykauf, K., Salek, M., Bomke, J., Frech, M., Lehmann, W. D., Dürst, M., and Alonso, A. (2006) Ubiquitin protein ligase Nedd4 binds to connexin43 by a phosphorylation-modulated process. *J. Cell Sci.* **119**, 3634–3642
  14. Kurata, W. E., and Lau, A. F. (1994) p130gag-fps disrupts gap junctional communication and induces phosphorylation of connexin43 in a manner similar to that of pp60v-src. *Oncogene* **9**, 329–335
  15. Filson, A. J., Azarnia, R., Beyers, E. C., Loewenstein, W. R., and Brugge, J. S. (1990) Tyrosine phosphorylation of a gap junction protein correlates with inhibition of cell-to-cell communication. *Cell Growth Differ.* **1**, 661–668
  16. Loo, L. W., Berestecky, J. M., Kanemitsu, M. Y., and Lau, A. F. (1995) pp60src-mediated phosphorylation of connexin 43, a gap junction protein. *J. Biol. Chem.* **270**, 12751–12761
  17. Kanemitsu, M. Y., Loo, L. W., Simon, S., Lau, A. F., and Eckhart, W. (1997) Tyrosine phosphorylation of connexin 43 by v-Src is mediated by SH2 and SH3 domain interactions. *J. Biol. Chem.* **272**, 22824–22831
  18. Azarnia, R., Reddy, S., Kmiecik, T. E., Shalloway, D., and Loewenstein, W. R. (1988) The cellular src gene product regulates junctional cell-to-cell communication. *Science* **239**, 398–401
  19. Firmbach-Kraft, I., Byers, M., Shows, T., Dalla-Favera, R., and Krolewski, J. J. (1990) *tyk2*, prototype of a novel class of non-receptor tyrosine kinase genes. *Oncogene* **5**, 1329–1336
  20. Strobl, B., Stoiber, D., Sexl, V., and Mueller, M. (2011) Tyrosine kinase 2 (TYK2) in cytokine signalling and host immunity. *Front. Biosci.* **16**, 3214–3232
  21. Wallweber, H. J., Tam, C., Franke, Y., Starovasnik, M. A., and Lupardus, P. J. (2014) Structural basis of recognition of interferon- $\alpha$  receptor by tyrosine kinase 2. *Nat. Struct. Mol. Biol.* **21**, 443–448
  22. Ghoreschi, K., Laurence, A., and O'Shea, J. J. (2009) Janus kinases in immune cell signaling. *Immunol. Rev.* **228**, 273–287
  23. Stark, G. R., and Darnell, J. E., Jr. (2012) The JAK-STAT pathway at twenty. *Immunity* **36**, 503–514
  24. Leonard, W. J. (2001) Role of Jak kinases and STATs in cytokine signal transduction. *Int. J. Hematol.* **73**, 271–277
  25. Minegishi, Y., Saito, M., Morio, T., Watanabe, K., Agematsu, K., Tsuchiya, S., Takada, H., Hara, T., Kawamura, N., Ariga, T., Kaneko, H., Kondo, N., Tsuge, I., Yachie, A., Sakiyama, Y., et al. (2006) Human tyrosine kinase 2 deficiency reveals its requisite roles in multiple cytokine signals involved in innate and acquired immunity. *Immunity* **25**, 745–755
  26. Karaghiosoff, M., Neubauer, H., Lassnig, C., Kovarik, P., Schindler, H., Pircher, H., McCoy, B., Bogdan, C., Decker, T., Brem, G., Pfeffer, K., and Müller, M. (2000) Partial impairment of cytokine responses in Tyk2-deficient mice. *Immunity* **13**, 549–560
  27. Wan, J., Fu, A. K., Ip, F. C., Ng, H. K., Hugon, J., Page, G., Wang, J. H., Lai, K. O., Wu, Z., and Ip, N. Y. (2010) Tyk2/STAT3 signaling mediates  $\beta$ -amyloid-induced neuronal cell death: implications in Alzheimer's disease. *J. Neurosci.* **30**, 6873–6881
  28. Sato, K., Shiota, M., Fukuda, S., Iwamoto, E., Machida, H., Inamine, T., Kondo, S., Yanagihara, K., Isomoto, H., Mizuta, Y., Kohno, S., and Tsukamoto, K. (2009) Strong evidence of a combination polymorphism of the tyrosine kinase 2 gene and the signal transducer and activator of transcription 3 gene as a DNA-based biomarker for susceptibility to Crohn's disease in the Japanese population. *J. Clin. Immunol.* **29**, 815–825
  29. Übel, C., Graser, A., Koch, S., Rieker, R. J., Lehr, H. A., Müller, M., and Finotto, S. (2014) Role of Tyk-2 in Th9 and Th17 cells in allergic asthma. *Sci. Rep.* **4**, 5865
  30. Marrero, M. B., Schieffer, B., Paxton, W. G., Duff, J. L., Berk, B. C., and Bernstein, K. E. (1995) The role of tyrosine phosphorylation in angiotensin II-mediated intracellular signalling. *Cardiovasc. Res.* **30**, 530–536
  31. Kodama, H., Fukuda, K., Pan, J., Makino, S., Sano, M., Takahashi, T., Hori, S., and Ogawa, S. (1998) Biphasic activation of the JAK/STAT pathway by angiotensin II in rat cardiomyocytes. *Circ. Res.* **82**, 244–250
  32. Yoon, N., Cho, J. G., Kim, K. H., Park, K. H., Sim, D. S., Yoon, H. J., Hong, Y. J., Park, H. W., Kim, J. H., Ahn, Y., Jeong, M. H., and Park, J. C. (2013) Beneficial effects of an angiotensin-II receptor blocker on structural atrial reverse-remodeling in a rat model of ischemic heart failure. *Exp. Ther. Med.* **5**, 1009–1016
  33. Pan, J., Fukuda, K., Saito, M., Matsuzaki, J., Kodama, H., Sano, M., Takahashi, T., Kato, T., and Ogawa, S. (1999) Mechanical stretch activates the JAK/STAT pathway in rat cardiomyocytes. *Circ. Res.* **84**, 1127–1136
  34. Pan, J., Fukuda, K., Kodama, H., Makino, S., Takahashi, T., Sano, M., Hori, S., and Ogawa, S. (1997) Role of angiotensin II in activation of the JAK/STAT pathway induced by acute pressure overload in the rat heart. *Circ. Res.* **81**, 611–617
  35. Lonn, E. M., Yusuf, S., Jha, P., Montague, T. J., Teo, K. K., Benedict, C. R., and Pitt, B. (1994) Emerging role of angiotensin-converting enzyme inhibitors in cardiac and vascular protection. *Circulation* **90**, 2056–2069
  36. Pagliaro, P., and Penna, C. (2005) Rethinking the renin-angiotensin system and its role in cardiovascular regulation. *Cardiovasc. Drugs Ther.* **19**, 77–87
  37. Akar, F. G., Spragg, D. D., Tunin, R. S., Kass, D. A., and Tomaselli, G. F. (2004) Mechanisms underlying conduction slowing and arrhythmogenesis in nonischemic dilated cardiomyopathy. *Circ. Res.* **95**, 717–725
  38. The SOLVD Investigators (1991) Effect of enalapril on survival in patients with reduced left ventricular ejection fractions and congestive heart failure. *N. Engl. J. Med.* **325**, 293–302
  39. Pfeffer, M. A., Braunwald, E., Moyé, L. A., Basta, L., Brown, E. J., Jr., Cuddy, T. E., Davis, B. R., Geltman, E. M., Goldman, S., and Flaker, G. C. (the SAVE Investigators) (1992) Effect of captopril on mortality and morbidity in patients with left ventricular dysfunction after myocardial infarction: results of the survival and ventricular enlargement trial. *N. Engl. J. Med.* **327**, 669–677
  40. Kasi, V. S., Xiao, H. D., Shang, L. L., Iravanian, S., Langberg, J., Witham, E. A., Jiao, Z., Gallego, C. J., Bernstein, K. E., and Dudley, S. C., Jr. (2007) Cardiac-restricted angiotensin-converting enzyme overexpression causes conduction defects and connexin dysregulation. *Am. J. Physiol. Heart Circ. Physiol.* **293**, H182–H192
  41. Tan, L. L., Li, L., Liu, L. M., and Zhao, H. L. (2013) Effect of RAAS antagonist on the expression of gap junction cx43 in myocardium of spontaneously hypertensive rat. *Sichuan Da Xue Xue Bao Yi Xue Ban* **44**, 531–535, 549
  42. Wang, R., Wang, Y., Lin, W. K., Zhang, Y., Liu, W., Huang, K., Terrar, D. A., Solaro, R. J., Wang, X., Ke, Y., and Lei, M. (2014) Inhibition of angiotensin II-induced cardiac hypertrophy and associated ventricular arrhythmias by a p21 activated kinase 1 bioactive peptide. *PLoS One* **9**, e101974
  43. Emdad, L., Uzzaman, M., Takagishi, Y., Honjo, H., Uchida, T., Severs, N. J., Kodama, I., and Murata, Y. (2001) Gap junction remodeling in hypertrophied left ventricles of aortic-banded rats: prevention by angiotensin II type 1 receptor blockade. *J. Mol. Cell. Cardiol.* **33**, 219–231
  44. Hussain, W., Patel, P. M., Chowdhury, R. A., Cabo, C., Ciaccio, E. J., Lab, M. J., Duffy, H. S., Wit, A. L., and Peters, N. S. (2010) The renin-angiotensin system mediates the effects of stretch on conduction velocity, connexin43 expression, and redistribution in intact ventricle. *J. Cardiovasc. Electrophysiol.* **21**, 1276–1283
  45. Kieken, F., Mutsaers, N., Dolmatova, E., Virgil, K., Wit, A. L., Kellezi, A., Hirst-Jensen, B. J., Duffy, H. S., and Sorgen, P. L. (2009) Structural and

- molecular mechanisms of gap junction remodeling in epicardial border zone myocytes following myocardial infarction. *Circ. Res.* **104**, 1103–1112
46. Sorgen, P. L., Duffy, H. S., Sahoo, P., Coombs, W., Delmar, M., and Spray, D. C. (2004) Structural changes in the carboxyl terminus of the gap junction protein connexin43 indicates signaling between binding domains for c-Src and zonula occludens-1. *J. Biol. Chem.* **279**, 54695–54701
  47. Delmar, M., and Makita, N. (2012) Cardiac connexins, mutations, and arrhythmias. *Curr. Opin. Cardiol.* **27**, 236–241
  48. Palatinus, J. A., Rhett, J. M., and Gourdie, R. G. (2012) The connexin43 carboxyl terminus and cardiac gap junction organization. *Biochim. Biophys. Acta* **1818**, 1831–1843
  49. Cooper, C. D., Solan, J. L., Dolejsi, M. K., and Lampe, P. D. (2000) Analysis of connexin phosphorylation sites. *Methods* **20**, 196–204
  50. Huang, Q. Y., Chen, Y. C., and Liu, S. P. (2012) Connexin 43, angiotensin II, endothelin 1, and type III collagen alterations in heart of rats having undergone fatal electrocution. *Am. J. Forensic Med. Pathol.* **33**, 215–221
  51. Solan, J. L., and Lampe, P. D. (2008) Connexin 43 in LA-25 cells with active v-src is phosphorylated on Tyr-247, Tyr-265, S262, S279/282, and S368 via multiple signaling pathways. *Cell Commun. Adhes.* **15**, 75–84
  52. Mitra, S. S., Xu, J., and Nicholson, B. J. (2012) Coregulation of multiple signaling mechanisms in pp60v-src-induced closure of Cx43 gap junction channels. *J. Membr. Biol.* **245**, 495–506
  53. Matesic, D. F., Rupp, H. L., Bonney, W. J., Ruch, R. J., and Trosko, J. E. (1994) Changes in gap-junction permeability, phosphorylation, and number mediated by phorbol ester and non-phorbol-ester tumor promoters in rat liver epithelial cells. *Mol. Carcinog.* **10**, 226–236
  54. Crow, D. S., Beyer, E. C., Paul, D. L., Kobe, S. S., and Lau, A. F. (1990) Phosphorylation of connexin43 gap junction protein in uninfected and Rous sarcoma virus-transformed mammalian fibroblasts. *Mol. Cell. Biol.* **10**, 1754–1763
  55. Sirnes, S., Leithe, E., and Rivedal, E. (2008) The detergent resistance of Connexin43 is lost upon TPA or EGF treatment and is an early step in gap junction endocytosis. *Biochem. Biophys. Res. Commun.* **373**, 597–601
  56. Musil, L. S., and Goodenough, D. A. (1991) Biochemical analysis of connexin43 intracellular transport, phosphorylation, and assembly into gap junctional plaques. *J. Cell Biol.* **115**, 1357–1374
  57. Zhou, L., Kasperek, E. M., and Nicholson, B. J. (1999) Dissection of the molecular basis of pp60(v-src) induced gating of connexin 43 gap junction channels. *J. Cell Biol.* **144**, 1033–1045
  58. Atkinson, M. M., Menko, A. S., Johnson, R. G., Sheppard, J. R., and Sheridan, J. D. (1981) Rapid and reversible reduction of junctional permeability in cells infected with a temperature-sensitive mutant of avian sarcoma virus. *J. Cell Biol.* **91**, 573–578
  59. Swenson, K. I., Piwnica-Worms, H., McNamee, H., and Paul, D. L. (1990) Tyrosine phosphorylation of the gap junction protein connexin43 is required for the pp60v-src-induced inhibition of communication. *Cell Regul.* **1**, 989–1002
  60. Lin, R., Warn-Cramer, B. J., Kurata, W. E., and Lau, A. F. (2001) v-Src-mediated phosphorylation of connexin43 on tyrosine disrupts gap junctional communication in mammalian cells. *Cell Commun. Adhes.* **8**, 265–269
  61. Murakami, Y., Nakano, S., Niho, Y., Hamasaki, N., and Izuhara, K. (1998) Constitutive activation of Jak-2 and Tyk-2 in a v-Src-transformed human gallbladder adenocarcinoma cell line. *J. Cell. Physiol.* **175**, 220–228
  62. Smyth, J. W., Hong, T. T., Gao, D., Vogan, J. M., Jensen, B. C., Fong, T. S., Simpson, P. C., Stainier, D. Y., Chi, N. C., and Shaw, R. M. (2010) Limited forward trafficking of connexin 43 reduces cell-cell coupling in stressed human and mouse myocardium. *J. Clin. Invest.* **120**, 266–279
  63. Alberts, B., Johnson, A., Lewis, J., Raff, M., Roberts, K., and Walter, P. (eds) (2002) Transport from the trans Golgi network to lysosomes, in *Molecular Biology of the Cell*, 4th Ed., Garland Science, New York
  64. Girão, H., Catarino, S., and Pereira, P. (2009) Eps15 interacts with ubiquitinated Cx43 and mediates its internalization. *Exp. Cell Res.* **315**, 3587–3597
  65. Lampe, P. D. (1994) Analyzing phorbol ester effects on gap junctional communication: a dramatic inhibition of assembly. *J. Cell Biol.* **127**, 1895–1905
  66. Lampe, P. D., TenBroek, E. M., Burt, J. M., Kurata, W. E., Johnson, R. G., and Lau, A. F. (2000) Phosphorylation of connexin43 on serine368 by protein kinase C regulates gap junctional communication. *J. Cell Biol.* **149**, 1503–1512
  67. Sáez, J. C., Nairn, A. C., Czernik, A. J., Fishman, G. I., Spray, D. C., and Hertzberg, E. L. (1997) Phosphorylation of connexin43 and the regulation of neonatal rat cardiac myocyte gap junctions. *J. Mol. Cell. Cardiol.* **29**, 2131–2145
  68. Park, D. J., Wallick, C. J., Martyn, K. D., Lau, A. F., Jin, C., and Warn-Cramer, B. J. (2007) Akt phosphorylates Connexin43 on Ser373, a “mode-1” binding site for 14–3-3. *Cell Commun. Adhes.* **14**, 211–226
  69. Nakazawa, T., Komai, S., Tezuka, T., Hisatsune, C., Umemori, H., Semba, K., Mishina, M., Manabe, T., and Yamamoto, T. (2001) Characterization of Fyn-mediated tyrosine phosphorylation sites on GluR  $\epsilon$ 2 (NR2B) subunit of the N-methyl-D-aspartate receptor. *J. Biol. Chem.* **276**, 693–699
  70. Hayashi, T., Thomas, G. M., and Haganir, R. L. (2009) Dual palmitoylation of NR2 subunits regulates NMDA receptor trafficking. *Neuron* **64**, 213–226
  71. Yang, K., Trepanier, C., Sidhu, B., Xie, Y. F., Li, H., Lei, G., Salter, M. W., Orser, B. A., Nakazawa, T., Yamamoto, T., Jackson, M. F., and Macdonald, J. F. (2012) Metaplasticity gated through differential regulation of GluN2A versus GluN2B receptors by Src family kinases. *EMBO J.* **31**, 805–816
  72. Stein, M., van Veen, T. A., Remme, C. A., Boulaksil, M., Noorman, M., van Stuijvenberg, L., van der Nagel, R., Bezzina, C. R., Hauer, R. N., de Bakker, J. M., and van Rijen, H. V. (2009) Combined reduction of intercellular coupling and membrane excitability differentially affects transverse and longitudinal cardiac conduction. *Cardiovasc. Res.* **83**, 52–60
  73. Alonso, F., Krattinger, N., Mazzolai, L., Simon, A., Waeber, G., Meda, P., and Haefliger, J. A. (2010) An angiotensin II- and NF- $\kappa$ B-dependent mechanism increases connexin 43 in murine arteries targeted by renin-dependent hypertension. *Cardiovasc. Res.* **87**, 166–176
  74. Fischer, R., Dechend, R., Gapelyuk, A., Shagdarsuren, E., Gruner, K., Gruner, A., Gratzke, P., Qadri, F., Wellner, M., Fiebeler, A., Dietz, R., Luft, F. C., Muller, D. N., and Schirdewan, A. (2007) Angiotensin II-induced sudden arrhythmic death and electrical remodeling. *Am. J. Physiology Heart Circ. Physiol.* **293**, H1242–H1253
  75. Kostin, S., Dammer, S., Hein, S., Klovekorn, W. P., Bauer, E. P., and Schaper, J. (2004) Connexin 43 expression and distribution in compensated and decompensated cardiac hypertrophy in patients with aortic stenosis. *Cardiovasc. Res.* **62**, 426–436
  76. Ozog, M. A., Bernier, S. M., Bates, D. C., Chatterjee, B., Lo, C. W., and Naus, C. C. (2004) The complex of ciliary neurotrophic factor-ciliary neurotrophic factor receptor  $\alpha$  up-regulates connexin43 and intercellular coupling in astrocytes via the Janus tyrosine kinase/signal transducer and activator of transcription pathway. *Mol. Biol. Cell* **15**, 4761–4774
  77. Xiong, H., Hong, J., Du, W., Lin, Y. W., Ren, L. L., Wang, Y. C., Su, W. Y., Wang, J. L., Cui, Y., Wang, Z. H., and Fang, J. Y. (2012) Roles of STAT3 and ZEB1 proteins in E-cadherin down-regulation and human colorectal cancer epithelial-mesenchymal transition. *J. Biol. Chem.* **287**, 5819–5832
  78. Govindarajan, R., Chakraborty, S., Johnson, K. E., Falk, M. M., Wheelock, M. J., Johnson, K. R., and Mehta, P. P. (2010) Assembly of connexin43 into gap junctions is regulated differentially by E-cadherin and N-cadherin in rat liver epithelial cells. *Mol. Biol. Cell* **21**, 4089–4107
  79. Axelsen, L. N., Stahlhut, M., Mohammed, S., Larsen, B. D., Nielsen, M. S., Holstein-Rathlou, N. H., Andersen, S., Jensen, O. N., Hennan, J. K., and Kjølbye, A. L. (2006) Identification of ischemia-regulated phosphorylation sites in connexin43: a possible target for the antiarrhythmic peptide analogue rotigaptide (ZP123). *J. Mol. Cell. Cardiol.* **40**, 790–798
  80. Cooper, C. D., and Lampe, P. D. (2002) Casein kinase 1 regulates connexin-43 gap junction assembly. *J. Biol. Chem.* **277**, 44962–44968
  81. Lampe, P. D., Cooper, C. D., King, T. J., and Burt, J. M. (2006) Analysis of Connexin43 phosphorylated at S325, S328, and S330 in normoxic and ischemic heart. *J. Cell Sci.* **119**, 3435–3442
  82. Mehta, P. P., Hotz-Wagenblatt, A., Rose, B., Shalloway, D., and Loewen-

## Tyk2 Phosphorylates Cx43

- stein, W. R. (1991) Incorporation of the gene for a cell-cell channel protein into transformed cells leads to normalization of growth. *J. Membr. Biol.* **124**, 207–225
83. Bolte, S., and Cordelières, F. P. (2006) A guided tour into subcellular colocalization analysis in light microscopy. *J. Microsc.* **224**, 213–232
84. Duffy, H. S., Sorgen, P. L., Girvin, M. E., O'Donnell, P., Coombs, W., Taffet, S. M., Delmar, M., and Spray, D. C. (2002) pH-dependent intramolecular binding and structure involving Cx43 cytoplasmic domains. *J. Biol. Chem.* **277**, 36706–36714
85. Breitkopf, S. B., and Asara, J. M. (2012) Determining *in vivo* phosphorylation sites using mass spectrometry. *Curr. Protoc. Mol. Biol.* 10.1002/0471142727.mb1819s98
86. Schneider, C. A., Rasband, W. S., and Eliceiri, K. W. (2012) NIH Image to ImageJ: 25 years of image analysis. *Nat. Methods* **9**, 671–675
87. Mitra, S., Annamalai, L., Chakraborty, S., Johnson, K., Song, X. H., Batra, S. K., and Mehta, P. P. (2006) Androgen-regulated formation and degradation of gap junctions in androgen-responsive human prostate cancer cells. *Mol. Biol. Cell* **17**, 5400–5416
88. Johnson, K. E., Mitra, S., Katoch, P., Kelsey, L. S., Johnson, K. R., and Mehta, P. P. (2013) Phosphorylation on Ser-279 and Ser-282 of connexin43 regulates endocytosis and gap junction assembly in pancreatic cancer cells. *Mol. Biol. Cell* **24**, 715–733
89. Marone, M., Mozzetti, S., De Ritis, D., Pierelli, L., and Scambia, G. (2001) Semiquantitative RT-PCR analysis to assess the expression levels of multiple transcripts from the same sample. *Biological Procedures Online* **3**, 19–25
90. Savitski, M. M., Lemeer, S., Boesche, M., Lang, M., Mathieson, T., Bantscheff, M., and Kuster, B. (2011) Confident phosphorylation site localization using the Mascot Delta Score. *Mol. Cell. Proteomics* **10**, M110.003830